

cut transversely, traced, and the areas determined. Approximately 100 myocytes were counted per mouse (n=12–13/group).

Morphometric analysis was also performed on aortic sections stained with Masson's trichrome to calculate the extent of perivascular fibrosis. The aorta and its surrounding collagen layer were traced, and the extent of fibrosis calculated by determining the percentage of the total area occupied by collagen (stained blue; n=10–12/group).

qRT-PCR

Aortas harvested from subject mice were snap frozen in liquid nitrogen (n=6–11/group). Excess tissue was removed under a dissecting microscope. RNA was isolated using the Qiagen RNeasy Mini Kit (Qiagen, Valencia, CA) using the manufacturer's protocol. cDNA was generated from the RNA using the qScript cDNA Supermix (Quanta Biosciences, Gaithersburg, MD). Quantitative real-time PCR was performed using the SsoAdvanced SYBR Green Supermix (Biorad, Hercules, CA) along with primers for PAI-1 (F: 5'-ACGCCTGGTGTGCTGGAATGC-3' and R: 5'-ACGGTGTGCCATCAGACTTGTG-3'), p16^{INK4a} (F: 5'-AGGGCCGTGTGCATGACGTG-3' and R: 5'-GCACCGGGC GGGAGAAGGTA-3'), and GAPDH (F: 5'-ATGTTCCAGTATGAC TCCACTCACG-3' and R: 5'-GAAGACACCAGTAGACTCCAC GACA-3'; Integrated DNA Technologies, Inc., Coralville, IA).

Average Telomere Length Ratio Quantification

Aortas and livers harvested from subject mice were snap frozen in liquid nitrogen (n=6–11/group). Excess tissue was removed under a dissecting microscope. Genomic DNA was isolated using the Qiagen DNeasy Blood & Tissue Kit (Qiagen, Valencia, CA) by following the manufacturer's protocol, and then was used to measure telomere length by quantitative real-time PCR as previously described with minor modification.^{29,30} Briefly, telomere repeats are amplified using specially designed primers, which are then compared with the amplification of a single-copy gene, the 36B4 gene (acidic ribosomal phosphoprotein PO), to determine the average telomere length ratio (ATLR). Either 15 ng (aortas) or 100 ng (livers) of genomic DNA template was added to each 20- μ l reaction containing forward and reverse primers (250 nmol/L each for telomere primers, and 500 nmol/L each for the 36B4 primers), SsoAdvanced SYBR Green Supermix (Biorad, Hercules, CA), and nuclease free water. A serially diluted standard curve of 25 ng to 1.5625 ng (aortas) or 100 ng to 3.125 ng (livers) per well of template DNA from a WT mouse sample was included on each plate for both the telomere and the 36B4 reactions to facilitate ATLR calculation. Ct values were converted to ng values according to the standard curves, and ng values of the telomere (T) reaction were divided by the ng values of the 36B4 (S) reaction to yield the ATLR. The primer sequences for the telomere portion were as follows: 5'-CGGTTTGGTTGGGTTTGGGTTTGGGTTTGGGTTTGGGTTTGGGTT-3' and 5'-GGCTTGCCTTACCCTTACCCTTACCCTTACCCTTACCCTTACCCT-3'. The primer sequences for the 36B4 single copy gene portion were as follows: 5'-ACTGGTCTAGGACC CGAGAAG-3' and 5'-TCAATGGTGCCTCTGGAGATT-3'. Cycling conditions for both primer sets (run in the same plate) were as follows: 95°C for 10 min, 30 cycles of 95°C for 15 s, and 55°C for 1 min for annealing and extension.

Statistical Analysis

All results are presented as mean \pm SD. Comparisons between 2 groups were tested by an unpaired, 2-tailed Student *t* test (unless otherwise noted). Results with *P*≤0.05 were considered significant.

Expanded methods and materials are available in the online-only Data Supplement.

Results

Generation and Validation of TM5441

TM5441 (molecular weight, 428.8 g/mol; cLogP, 3.319) was discovered through an extensive structure-activity relationship study with more than 170 novel derivatives with comparatively low molecular weights (400 to 550 g/mol) and without

symmetrical structure, designed on the basis of the original lead compound TM5007¹⁹ and an already successful modified version, TM5275.¹⁸ TM5007 was identified virtually by structure-based drug design after undergoing a docking simulation that selected for compounds that fit within the cleft of PAI-1 (s3A in the human PAI-1 3-dimensional structure) accessible to insertion of the reactive center loop. Compounds that bind in this cleft would block reactive center loop insertion and thus prevent PAI-1 activity. Once TM5007 had been identified as a PAI-1 inhibitor both virtually and in vitro/in vivo, further compounds were derived via chemical modification to improve the pharmacokinetic properties of the inhibitor, resulting in the generation of TM5275 and later TM5441 (Table). The inhibitory activity of TM5441 was shown in vitro by a chromogenic assay (Figure 1A and 1B), and its specificity was confirmed by demonstrating that it did not inhibit other SERPINS such as antithrombin III (Figure 1C) and α 2-antiplasmin (Figure 1D).

TM5441 Attenuates the Effects of L-NAME on Systolic Blood Pressure

Six- to 8-week-old WT C57BL/6J animals were given either L-NAME (1 mg/mL) water or regular water for 8 weeks. Additionally, animals received either TM5441 (20 mg/kg/day) chow or regular diet. Systolic blood pressure (SBP) was measured every 2 weeks over the course of the study. As shown in Figure 2A, animals given L-NAME in their drinking water for 8 weeks had a 35% increase in SBP compared with WT animals receiving untreated water (183 \pm 13 mmHg vs 135 \pm 16 mmHg, *P*=3.1 \times 10⁻⁷). However, animals receiving both L-NAME and the PAI-1 inhibitor TM5441 had significantly lower SBPs compared with those that received L-NAME alone (163 \pm 21 mmHg vs 183 \pm 13 mmHg, *P*=0.009). This difference in SBP between L-NAME and L-NAME+TM5441 animals was similar to previously reported data comparing L-NAME-treated WT and PAI-1-deficient mice.^{16,17} Thus, we confirmed that pharmacologic inhibition of PAI-1 activity using the novel antagonist TM5441 protects against L-NAME-induced hypertension to a similar degree as the full genetic knockout. As a control, we also looked at animals receiving only TM5441 to show that the drug had no off-target effects on SBP. These animals showed no difference in SBP compared with WT. Additionally, using LC/MS/MS, we confirmed the presence of TM5441 in the plasma of our cotreated animals and showed that the concentration of TM5441 correlated slightly with SBP (Figure I in the online-only Data Supplement).

TM5441 Reduces Cardiac Hypertrophy Derived From L-NAME Treatment

As shown in Figure 2B, L-NAME-treated animals showed a significant thickening of their left ventricle anterior wall during diastole relative to WT (1.00 \pm 0.11 mm vs 0.86 \pm 0.11 mm,

Table. Pharmacokinetic Properties of PAI-1 Inhibitors

Inhibitor	Oral Dose in Rat	C _{max} (μ mol/L)	T _{max} (h)	T _{1/2} (h)
TM5007 ¹⁸	50 mg/kg	8.8	18	124
TM5275 ¹⁸	50 mg/kg	34	2	2.5
TM5441	5 mg/kg	17.9	1	2.3

C_{max} indicates maximum drug concentration; T_{1/2}, drug half-life; and T_{max}, maximum drug concentration time.

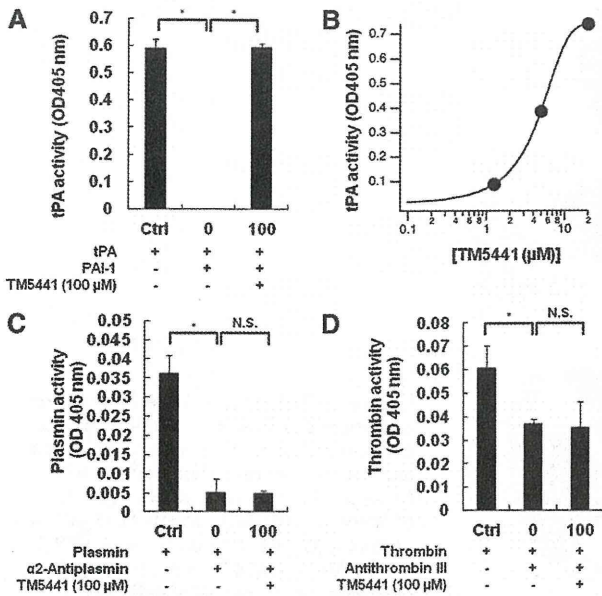


Figure 1. TM5441 specifically inhibits plasminogen activator inhibitor (PAI). **A** and **B**, TM5441 inhibited the PAI-1 activity in a dose-dependent manner, but did not modify other SERPIN/serine protease systems such as **(C)** α2-antiplasmin/plasmin and **(D)** antithrombin III/thrombin. Data are mean±SD. **P* < 0.01 by 1-way ANOVA and Dunnett test. n=3. N.S. indicates not significant; and tPA, tissue plasminogen activator.

P=0.006). PAI-1 antagonism attenuated left ventricle anterior wall thickness compared with L-NAME treatment alone (0.84±0.09 mm vs 1.00±0.11 mm, *P*=0.002). This reduction in cardiac hypertrophy was seen at the cellular level as well

(Figure 2C). Left ventricle myocyte cross-sectional area significantly increased in WT + L-NAME mice compared with WT (334±37 μm² vs 262±31 μm², *P*=0.00003), but cotreatment with TM5441 reduced the extent of hypertrophy compared with L-NAME treatment alone (300±42 μm² vs 334±37 μm², *P*=0.04). Animals receiving only TM5441 were not significantly different from WT in either measurement.

TM5441 Prevents the Development of Periaortic Fibrosis

Cross-sections from the aorta were stained with Masson trichrome to examine the extent of perivascular fibrosis. As shown in Figure 3, the ratio of fibrotic area compared with total vascular area was significantly increased in L-NAME-treated animals compared with WT (31±6 % vs 22±3%, *P*=0.0006). However, coadministration of TM5441 with L-NAME prevented collagen accumulation around the aorta so that these animals maintained a baseline level of fibrosis (21±3% vs 31±6% for WT + L-NAME, *P*=0.0006). Thus, PAI-1 inhibition prevents the structural remodeling of the vasculature associated with L-NAME treatment.

TM5441 Protects Against L-NAME-Induced Vascular Senescence

Previous *in vitro* work has demonstrated that the loss of NO through L-NAME treatment can lead to endothelial cell senescence.^{22,23} In this study, we determined the level of senescence *in vivo* in aortas using quantitative RT-PCR. When examining the senescence marker p16^{Ink4a}, we found that whereas L-NAME treatment significantly increased the expression of p16^{Ink4a} 3-fold (*P*=0.008 vs WT), this increase was prevented by

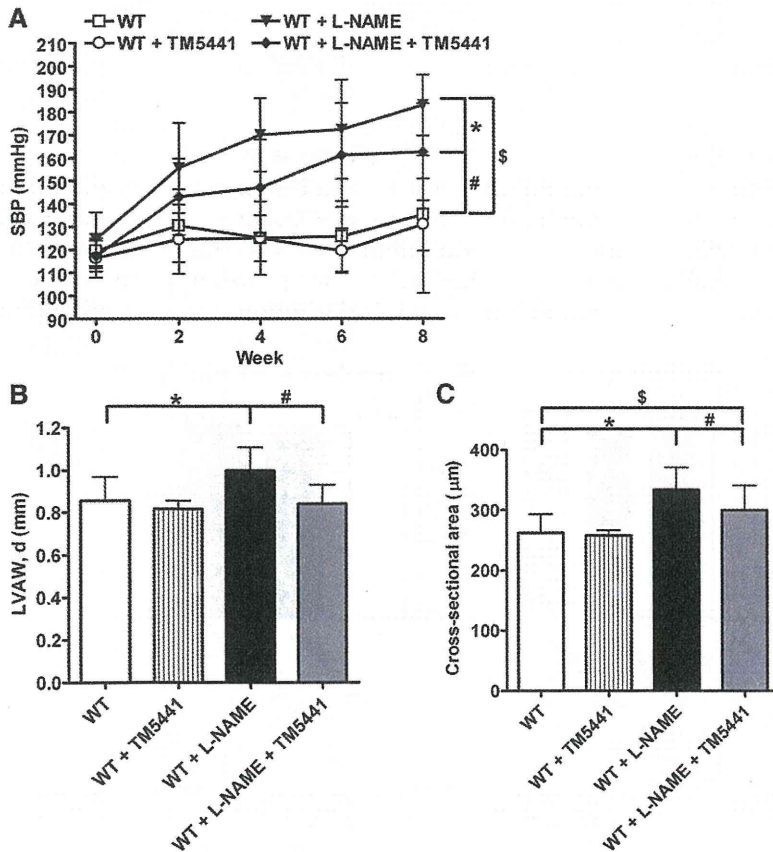


Figure 2. The effect of N^ω-nitro-L-arginine methyl ester (L-NAME) and TM5441 on hypertension and hypertrophy. **A**, Systolic blood pressure (SBP) was measured throughout the course of the study every 2 weeks. **P*=0.009, #*P*=0.001, \$*P*=3.1×10⁻⁷. **B**, Echocardiograms were performed on 8-week-old mice before sacrifice. Left ventricle anterior wall thickness (LVAW) was measured at diastole. **P*=0.006, #*P*=0.002. **C**, Left ventricles were cross-sectioned and stained using hematoxylin and eosin. Approximately 100 transversely cut myocytes per mouse were traced and cross-sectional area was quantified. **P*=0.04, #*P*=0.00003, \$*P*=0.01. Data are mean±SD. n=12–13. WT indicates wild type.

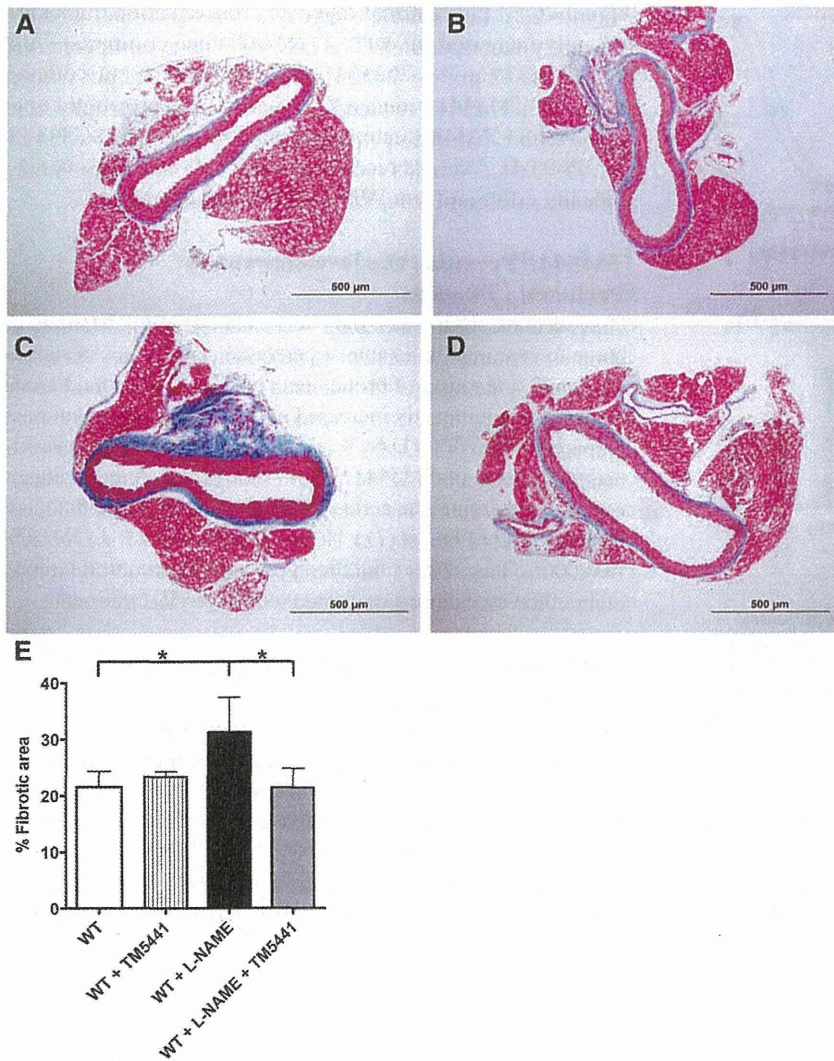


Figure 3. TM5441 attenuates N^o-nitro-L-arginine methyl ester (L-NAME)-induced periaortic fibrosis. Cross-sections of the aorta were sectioned and stained with Masson trichrome to evaluate the extent of fibrosis in (A) wild-type (WT), (B) WT + TM5441, (C) WT + L-NAME, and (D) WT + L-NAME + TM5441 mice. Blue staining indicates the presence of collagen. E, The ratio of fibrotic to total vascular area was calculated. **P*=0.006. Data are mean±SD. n=10–12.

TM5441 cotreatment (*P*=0.01 vs WT+L-NAME; Figure 4A). We confirmed these results by using a PCR method to measure ATLR in both liver (Figure 4B) and aorta (Figure 4C).^{29,30} In both tissues, L-NAME significantly reduced telomere length, whereas those animals receiving L-NAME and TM5441 had no change in telomere length relative to WT animals.

Discussion

Long-term NOS inhibition leads to hypertension through the combination of the loss of NO-dependent vasodilation and arteriosclerotic remodeling of the vasculature.⁵⁻⁷ Similar to previously reported data,^{16,17} in the present study SBP increased after only 2 weeks of L-NAME treatment and continued to rise

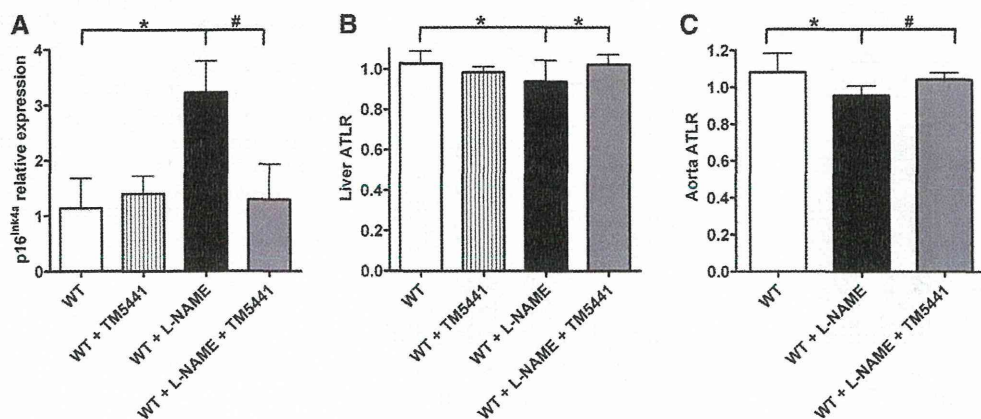


Figure 4. N^o-nitro-L-arginine methyl ester (L-NAME) induces vascular senescence. A, Expression levels of p16^{ink4a} mRNA normalized to GAPDH. **P*=0.008, #*P*=0.01. Average telomere length ratio (ATLR) for (B) livers and (C) aortas. B, **P*=0.02; C, **P*=0.01, #*P*=0.003. Data are mean±SD. n=6–11. WT indicates wild type.

throughout the study. However, when the animals were simultaneously treated with L-NAME and the PAI-1 inhibitor TM5441, the increase in SBP was blunted. This reduction in SBP is similar to that seen previously with PAI-1-deficient mice,^{16,17} indicating that TM5441 is effective in minimizing the effects of L-NAME on SBP. These results correlate with our previous observations that loss of PAI-1 is protective against angiotensin II-induced hypertension (Figure II in the online-only Data Supplement), thus demonstrating that the effect of PAI-1 on SBP is NO-independent. To our knowledge, this is the first instance of a non-antihypertensive drug successfully preventing systolic hypertension.

Left ventricular hypertrophy is a common consequence of hypertension. Accordingly, we used echocardiography and histology to evaluate the left ventricle in the experimental animals. L-NAME caused significant increases in both wall thickness and myocyte cross-sectional area. TM5441 treatment reduced these compensatory responses by 16% and 10%, respectively. This reduction in hypertrophy further demonstrates that PAI-1 inhibition effectively protects against hypertension and its associated pathologies.

In addition to the changes in blood pressure, we directly examined the changes in vascular remodeling caused by L-NAME by quantifying the extent of periaortic fibrosis in these animals. L-NAME-treated mice had almost 50% more fibrosis surrounding their aortas as compared with the aortas from untreated WT. This increase was completely attenuated in animals receiving both L-NAME and TM5441, as these mice had identical levels of fibrosis to that observed in untreated WT controls. Excess PAI-1 is known to exacerbate the development of fibrosis in a variety of animal models,^{31,32} and L-NAME elevates arterial PAI-1 expression.⁹ Furthermore, we have previously shown that PAI-1 deficiency both augments gelatinolytic activity in coronary arteries using *in situ* zymography¹⁷ and protects against periaortic fibrosis induced by angiotensin II.³³ Taken together, these data identify a mechanism through which PAI-1 deficiency is protective against collagen deposition and perivascular fibrosis. Thus, we would anticipate both the structural changes seen in the L-NAME-treated aortas and the protection against these changes provided by TM5441.

The capacity of TM5441 to prevent the increase in SBP and reduce the development of hypertrophy and arteriosclerosis makes it a promising therapeutic, particularly in the elderly population where arteriosclerosis likely makes a major contribution to this common malady. Even though TM5441 treatment did not fully attenuate the increase in SBP attributable to NOS inhibition, the almost complete prevention of periaortic fibrosis indicates that PAI-1 inhibition is a novel approach to combat the structural remodeling in clinical situations and conditions associated with reduced NO production or bioavailability.

Loss of NO production has been shown to induce vascular senescence *in vitro*,^{22,23} and increased PAI-1 is an established as a marker of senescence.^{24,25} However, little work has been done to examine the role of NO in senescence *in vivo*. We determined that NOS inhibition can induce senescence *in vivo* by showing that L-NAME-treated aortas had a 3-fold increase in expression of the senescence marker p16^{Ink4a} relative to WT controls. More importantly, we wanted to establish that PAI-1 is not just a marker of senescence, but rather is a critical driver of this process *in vivo*. This was confirmed by demonstrating that aortic p16^{Ink4a} levels in

mice treated with both L-NAME and TM5441 were comparable with those seen in WT controls. This observation is in agreement with other data from this laboratory indicating that partial or complete deficiency of PAI-1 in the *klotho* mouse model is sufficient to prevent senescence and prolong survival (M. Eren, manuscript under review). Telomere length, another well-established cellular marker of physiological aging, was also examined in both aortic and hepatic tissues. We chose to examine the liver because it is a highly vascularized organ and has been previously shown to be affected by L-NAME.³⁴ Both aortas and livers from L-NAME-treated animals showed significant decreases in ATLR that reflect the induction of senescence and accelerated aging. In both organs, cotreatment of L-NAME with TM5441 was able to maintain telomere length similar to WT levels.

The present study establishes PAI-1 as an important determinant of vascular senescence *in vivo*. Additionally, it is possible that all the pathological conditions developed in the L-NAME-treated animals (hypertension, perivascular fibrosis, and hypertrophy) could be secondary effects from the induction of vascular senescence. This is further supported by the fact that age is the single greatest risk factor for cardiovascular disease.^{35,36} PAI-1 expression is known to be both elevated in the elderly and in many conditions associated with aging such as obesity, insulin resistance, and vascular remodeling.³⁷ Furthermore, NO production has been shown to decrease with age, even in healthy individuals.³⁸ Combined with the data shown here, these findings indicate that age-related decreases in NO production can lead to vascular senescence and arteriosclerosis, and that this process may be prevented through PAI-1 inhibition. These findings certainly suggest that PAI-1 antagonists may eventually prove to be useful in preventing hypertension as well as protecting against the increased risk in cardiovascular disease that accompanies aging.

In conclusion, we have shown that TM5441, a novel, orally active PAI antagonist, protects mice against L-NAME-induced vascular pathologies, including hypertension, fibrosis, and vascular senescence. TM5441 represents a novel therapeutic approach for the aging-associated cardiovascular disease that merits further investigation.

Acknowledgments

We thank Marissa Michaels, MS for her help in obtaining reagents and Aaron Place, PhD and Varun Nagpal, MS for reviewing the manuscript.

Sources of Funding

This work was supported by National Institutes of Health (NIH)/National Heart, Lung, and Blood Institute (NHLBI) grants 2R01 HL051387 and 1P01HL108795.

Disclosures

None.

References

1. Knowles RG, Moncada S. Nitric oxide synthases in mammals. *Biochem J*. 1994;298 (Pt 2):249–258.
2. Féférou M, Köhler R, Vanhoutte PM. Nitric oxide: orchestrator of endothelium-dependent responses. *Ann Med*. 2012;44:694–716.
3. Huang PL, Huang Z, Mashimo H, Bloch KD, Moskowitz MA, Bevan JA, Fishman MC. Hypertension in mice lacking the gene for endothelial nitric oxide synthase. *Nature*. 1995;377:239–242.
4. Shesely EG, Maeda N, Kim HS, Desai KM, Krege JH, Laubach VE, Sherman PA, Sessa WC, Smithies O. Elevated blood pressures in mice

- lacking endothelial nitric oxide synthase. *Proc Natl Acad Sci USA*. 1996;93:13176–13181.
5. Zatz R, Baylis C. Chronic nitric oxide inhibition model six years on. *Hypertension*. 1998;32:958–964.
 6. Baylis C, Mitruka B, Deng A. Chronic blockade of nitric oxide synthesis in the rat produces systemic hypertension and glomerular damage. *J Clin Invest*. 1992;90:278–281.
 7. Ribeiro MO, Antunes E, de Nucci G, Lovisolo SM, Zatz R. Chronic inhibition of nitric oxide synthesis. A new model of arterial hypertension. *Hypertension*. 1992;20:298–303.
 8. Bouchie JL, Hansen H, Feener EP. Natriuretic factors and nitric oxide suppress plasminogen activator inhibitor-1 expression in vascular smooth muscle cells. Role of cGMP in the regulation of the plasminogen system. *Arterioscler Thromb Vasc Biol*. 1998;18:1771–1779.
 9. Katoh M, Egashira K, Mitsui T, Chishima S, Takeshita A, Narita H. Angiotensin-converting enzyme inhibitor prevents plasminogen activator inhibitor-1 expression in a rat model with cardiovascular remodeling induced by chronic inhibition of nitric oxide synthesis. *J Mol Cell Cardiol*. 2000;32:73–83.
 10. Vaughan DE. Plasminogen Activator Inhibitor 1: Molecular Aspects and Clinical Importance. *J Thromb Thrombolysis*. 1995;2:187–193.
 11. Stefansson S, Lawrence DA. The serpin PAI-1 inhibits cell migration by blocking integrin alpha V beta 3 binding to vitronectin. *Nature*. 1996;383:441–443.
 12. Heymans S, Lutun A, Nuyens D, Theilmeier G, Creemers E, Moons L, Dyspersin GD, Cleutjens JP, Shipley M, Angellilo A, Levi M, Nübe O, Baker A, Keshet E, Lupu F, Herbert JM, Smits JF, Shapiro SD, Baes M, Borgers M, Collen D, Daemen MJ, Carmeliet P. Inhibition of plasminogen activators or matrix metalloproteinases prevents cardiac rupture but impairs therapeutic angiogenesis and causes cardiac failure. *Nat Med*. 1999;5:1135–1142.
 13. Olman MA, Mackman N, Gladson CL, Moser KM, Loskutoff DJ. Changes in procoagulant and fibrinolytic gene expression during bleomycin-induced lung injury in the mouse. *J Clin Invest*. 1995;96:1621–1630.
 14. Oikawa T, Freeman M, Lo W, Vaughan DE, Fogo A. Modulation of plasminogen activator inhibitor-1 in vivo: a new mechanism for the anti-fibrotic effect of renin-angiotensin inhibition. *Kidney Int*. 1997;51:164–172.
 15. Eren M, Painter CA, Atkinson JB, Declerck PJ, Vaughan DE. Age-dependent spontaneous coronary arterial thrombosis in transgenic mice that express a stable form of human plasminogen activator inhibitor-1. *Circulation*. 2002;106:491–496.
 16. Kaikita K, Fogo AB, Ma L, Schoenhard JA, Brown NJ, Vaughan DE. Plasminogen activator inhibitor-1 deficiency prevents hypertension and vascular fibrosis in response to long-term nitric oxide synthase inhibition. *Circulation*. 2001;104:839–844.
 17. Kaikita K, Schoenhard JA, Painter CA, Ripley RT, Brown NJ, Fogo AB, Vaughan DE. Potential roles of plasminogen activator system in coronary vascular remodeling induced by long-term nitric oxide synthase inhibition. *J Mol Cell Cardiol*. 2002;34:617–627.
 18. Izuohara Y, Yamaoka N, Kodama H, Dan T, Takizawa S, Hirayama N, Meguro K, van Ypersele de Strihou C, Miyata T. A novel inhibitor of plasminogen activator inhibitor-1 provides antithrombotic benefits devoid of bleeding effect in nonhuman primates. *J Cereb Blood Flow Metab*. 2010;30:904–912.
 19. Izuohara Y, Takahashi S, Nangaku M, Takizawa S, Ishida H, Kurokawa K, van Ypersele de Strihou C, Hirayama N, Miyata T. Inhibition of plasminogen activator inhibitor-1: its mechanism and effectiveness on coagulation and fibrosis. *Arterioscler Thromb Vasc Biol*. 2008;28:672–677.
 20. Sato I, Morita I, Kaji K, Ikeda M, Nagao M, Murota S. Reduction of nitric oxide producing activity associated with *in vitro* aging in cultured human umbilical vein endothelial cell. *Biochem Biophys Res Commun*. 1993;195:1070–1076.
 21. Matsushita H, Chang E, Glassford AJ, Cooke JP, Chiu CP, Tsao PS. eNOS activity is reduced in senescent human endothelial cells: Preservation by hTERT immortalization. *Circ Res*. 2001;89:793–798.
 22. Hayashi T, Matsui-Hirai H, Miyazaki-Akita A, Fukatsu A, Funami J, Ding QF, Kamalanathan S, Hattori Y, Ignarro LJ, Iguchi A. Endothelial cellular senescence is inhibited by nitric oxide: implications in atherosclerosis associated with menopause and diabetes. *Proc Natl Acad Sci USA*. 2006;103:17018–17023.
 23. Zhong W, Zou G, Gu J, Zhang J. L-arginine attenuates high glucose-accelerated senescence in human umbilical vein endothelial cells. *Diabetes Res Clin Pract*. 2010;89:38–45.
 24. Kuilman T, Peeper DS. Senescence-messaging secretome: SMS-ing cellular stress. *Nat Rev Cancer*. 2009;9:81–94.
 25. Kortlever RM, Higgins PJ, Bernards R. Plasminogen activator inhibitor-1 is a critical downstream target of p53 in the induction of replicative senescence. *Nat Cell Biol*. 2006;8:877–884.
 26. Elzi DJ, Lai Y, Song M, Hakala K, Weintraub ST, Shiio Y. Plasminogen activator inhibitor 1–insulin-like growth factor binding protein 3 cascade regulates stress-induced senescence. *Proc Natl Acad Sci USA*. 2012;109:12052–12057.
 27. Izuohara Y, Takahashi S, Nangaku M, Takizawa S, Ishida H, Kurokawa K, van Ypersele de Strihou C, Hirayama N, Miyata T. Inhibition of plasminogen activator inhibitor-1: its mechanism and effectiveness on coagulation and fibrosis. *Arterioscler Thromb Vasc Biol*. 2008;28:672–677.
 28. Izuohara Y, Yamaoka N, Kodama H, Dan T, Takizawa S, Hirayama N, Meguro K, van Ypersele de Strihou C, Miyata T. A novel inhibitor of plasminogen activator inhibitor-1 provides antithrombotic benefits devoid of bleeding effect in nonhuman primates. *J Cereb Blood Flow Metab*. 2010;30:904–912.
 29. Cawthon RM. Telomere measurement by quantitative PCR. *Nucleic Acids Res*. 2002;30:e47.
 30. Callicott RJ, Womack JE. Real-time PCR assay for measurement of mouse telomeres. *Comp Med*. 2006;56:17–22.
 31. Eitzman DT, McCoy RD, Zheng X, Fay WP, Shen T, Ginsburg D, Simon RH. Bleomycin-induced pulmonary fibrosis in transgenic mice that either lack or overexpress the murine plasminogen activator inhibitor-1 gene. *J Clin Invest*. 1996;97:232–237.
 32. Eren M, Gleaves LA, Atkinson JB, King LE, Declerck PJ, Vaughan DE. Reactive site-dependent phenotypic alterations in plasminogen activator inhibitor-1 transgenic mice. *J Thromb Haemost*. 2007;5:1500–1508.
 33. Weisberg AD, Albormoz F, Griffin JP, Crandall DL, Elokda H, Fogo AB, Vaughan DE, Brown NJ. Pharmacological inhibition and genetic deficiency of plasminogen activator inhibitor-1 attenuates angiotensin II/salt-induced aortic remodeling. *Arterioscler Thromb Vasc Biol*. 2005;25:365–371.
 34. Smith LH, Dixon JD, Stringham JR, Eren M, Elokda H, Crandall DL, Washington K, Vaughan DE. Pivotal role of PAI-1 in a murine model of hepatic vein thrombosis. *Blood*. 2006;107:132–134.
 35. Najjar SS, Scuteri A, Lakatta EG. Arterial aging: is it an immutable cardiovascular risk factor? *Hypertension*. 2005;46:454–462.
 36. Jousilahti P, Vartiainen E, Tuomilehto J, Puska P. Sex, age, cardiovascular risk factors, and coronary heart disease: a prospective follow-up study of 14 786 middle-aged men and women in Finland. *Circulation*. 1999;99:1165–1172.
 37. Yamamoto K, Takeshita K, Kojima T, Takamatsu J, Saito H. Aging and plasminogen activator inhibitor-1 (PAI-1) regulation: implication in the pathogenesis of thrombotic disorders in the elderly. *Cardiovasc Res*. 2005;66:276–285.
 38. Lyons D, Roy S, Patel M, Benjamin N, Swift CG. Impaired nitric oxide-mediated vasodilatation and total body nitric oxide production in healthy old age. *Clin Sci*. 1997;93:519–525.

CLINICAL PERSPECTIVE

This research is the first to establish a role for NO and plasminogen activator inhibitor (PAI) in vascular senescence *in vivo*. We have shown that the inhibition of NO production and the resulting increase in vascular PAI-1 expression leads to arteriosclerosis and biochemical and molecular evidence of vascular senescence that can be attenuated with the specific PAI-1 antagonist TM5441. PAI-1 is known to be a key contributor in both fibrotic and thrombotic cardiovascular disease. By demonstrating that an orally active PAI-1 antagonist is effective at preventing N^o-nitro-L-arginine methyl ester (L-NAME)-induced vascular pathology, this research suggests the possibility that TM5441 could be used in the clinic to not only treat fibrotic and thrombotic disorders, but to also protect and defend vascular health overall. Furthermore, we know that age is the single greatest risk factor for cardiovascular disease, that PAI-1 levels increase with age, and that senescence and physiological aging are fundamentally linked. The use of PAI-1 antagonists thus emerges as a potential clinical tool to combat age-related vascular disease and arteriosclerosis.

SUPPLEMENTAL MATERIAL

Supplemental Methods

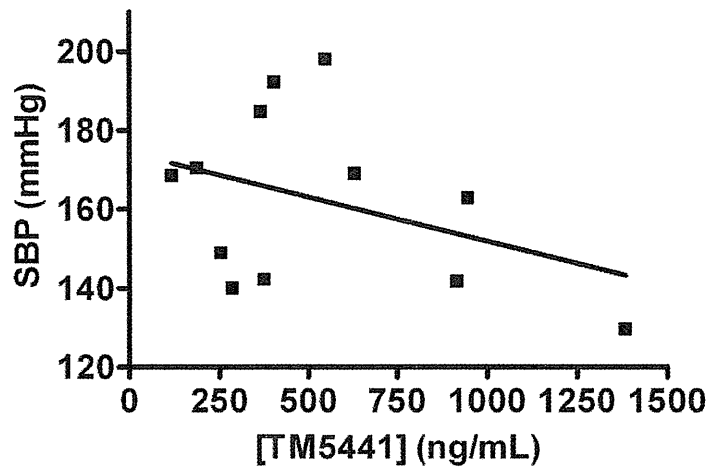
TM5441 LC/MS/MS: Samples were separated initially on a phenomenex column (C18, 1.7 μ m, 2.1 x 50 mm column, Waters Corporation, Milford, Massachusetts, USA) run by a Shimadzu HPLC system (Shimadzu corp., Kyoto, Japan) using a gradient of acetonitrile (ACN) with 0.1% formic acid. Mass spectrometry detection was performed on an Applied Biosystems API-4000 MS/MS system (Applied-Biosystems, Foster City, California, USA) with an atmospheric pressure electrospray ionization source. Analyst 1.5 software packages were used to control the LC-MS/MS system, acquire data, and analysis. All analyses were carried out in positive ionization with spray voltage set at 5500 V. The heated capillary temperature was set at 550 °C. The curtain gas, ion source gas 1, ion source gas 2, entrance potential, collision exit potential, and declustering potential were set at 10, 55, 55, 10, 10, 70 Arb, respectively. The collision energy was set at 20 and 25 for TM5441 and IS, respectively. For quantification, multiple reactions monitoring (MRM) was utilized for the transitions 429.1 m/z \rightarrow 230.5 m/z for TM5441 and 429.1 m/z \rightarrow 230.5 m/z for IS.

A stock solution of TM5441, 1 mg/mL, was prepared in DMSO. TM5441 standard solutions that ranged from 50 ng/mL to 250,000 ng/mL were prepared by serial dilutions in DMSO. The indomethacin (IS) stock solution was prepared in ACN with a final concentration of 1 mg/mL. The calibration curve was prepared by spiking 10 μ L of the appropriate intermediate analytical standard into 490 μ L blank mouse plasma to yield a concentration range of 1 ng/mL to 5,000 ng/mL. The quality control (QC) samples were prepared similarly at concentrations of 10 ng/mL and 1,000 ng/mL in mouse plasma by separately weighed compound.

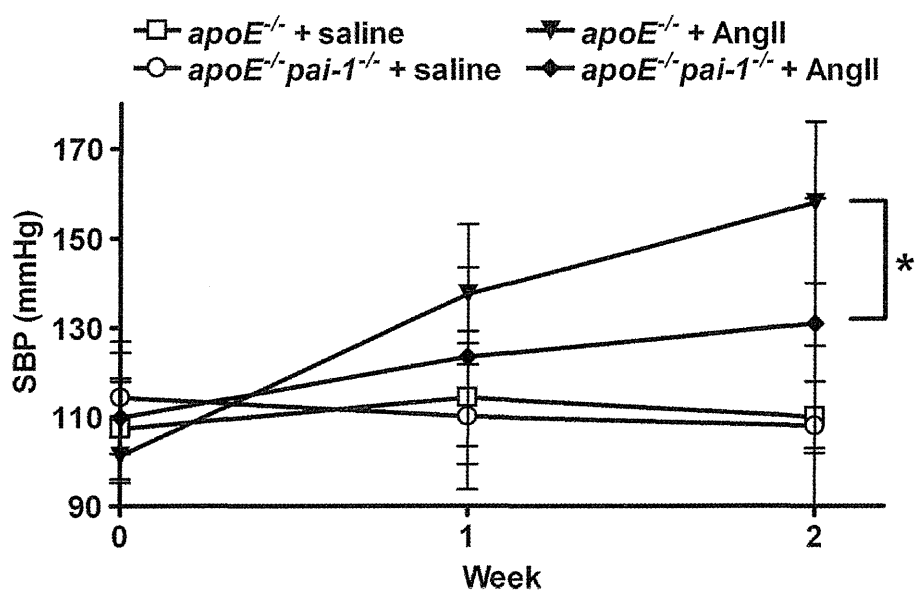
A 50 μ L aliquot of plasma was transferred to a 2 mL eppendorf micro centrifuge tube and 200 μ L of cold IS solution was added. For double blank samples, a 50 μ L aliquot of blank plasma was added to 200 μ L of cold ACN. The samples were then vortexed for 10 mins, followed by centrifugation at 14k rpms and 4°C for 10 mins and 100 μ L of supernatant was collected in a 96-well plate. A 2 μ L aliquot was injected into the LC-MS/MS system for analysis. The QC samples were injected after every six unknown samples.

Angiotensin II Blood Pressure: apoE^{-/-} and pai-1^{-/-} mice, both of which are in the C57BL/6J background, were purchased from Jackson Laboratories (Bar Harbor, ME) and then crossed to generate apoE^{-/-}pai-1^{-/-}. Saline and angiotensin II (AngII) solutions were infused into either apoE^{-/-} or apoE^{-/-}pai-1^{-/-} using osmotic minipumps (Alzet, type 1002, Durect Corporation, Cupertino, CA) that were implanted subcutaneously. Minipumps were loaded with Ang II resuspended in 0.9% sterile saline solution to deliver a dose of 600 ng/kg/min for 14 days. Mice in the control group received saline only. Systolic blood pressure was measured in conscious mice once a week using a non-invasive tail-cuff system (BP 2000, Visitech Systems, NC). Animals were habituated to the measurement conditions (under a restrainer on temperature controlled platform for up to one hour) for 3 days before recording the baseline measurements. Three sets of 10 measurements were recorded for each animal approximately at the same time of the day.

Supplemental Figures and Legends



Supplemental Figure 1. SBP as a function of plasma levels of TM5441. LC/MS/MS measurements were used to confirm the presence of TM5441 in the plasma from L-NAME-treated animals. The average concentration in the WT + L-NAME + TM5441 group was 535 ng/mL. The amount of TM5441 correlated with the reduction of SBP, though not significantly. $R^2 = 0.1448$.



Supplemental Figure 2. PAI-1 deficiency protects against angiotensin II-induced hypertension.

Mice were administered either angiotensin II (AngII) or saline via osmotic mini-pump for 2 weeks. PAI-1 deficiency attenuated the increase in SBP due to AngII. ApoE deficiency has no effect on SBP and should be regarded as identical to WT animals. Data are mean \pm SD. n=12.

*P=0.01.

Inhibition of Plasminogen Activator Inhibitor Type-1 Activity Enhances Rapid and Sustainable Hematopoietic Regeneration

ABD AZIZ IBRAHIM,^{a,b} TAKASHI YAHATA,^{a,c} MAKOTO ONIZUKA,^{a,b} TAKASHI DAN,^d CHARLES VAN YPERSELE DE STRIHOUE,^e TOSHIO MIYATA,^d KIYOSHI ANDO^{a,b}

Key Words. Hematopoietic stem cells • Bone marrow stromal cells • Hematopoiesis • Stem cell transplantation • Tissue regeneration • Osteoblast

ABSTRACT

The prognosis of patients undergoing hematopoietic stem cell transplantation (HSCT) depends on the rapid recovery and sustained life-long hematopoiesis. The activation of the fibrinolytic pathway promotes hematopoietic regeneration; however, the role of plasminogen activator inhibitor-1 (PAI-1), a negative regulator of the fibrinolytic pathway, has not yet been elucidated. We herein demonstrate that bone marrow (BM) stromal cells, especially osteoblasts, produce PAI-1 in response to myeloablation, which negatively regulates the hematopoietic regeneration in the BM microenvironment. Total body irradiation in mice dramatically increased the local expression levels of fibrinolytic factors, including tissue-type plasminogen activator (tPA), plasmin, and PAI-1. Genetic disruption of the *PAI-1* gene, or pharmacological inhibition of PAI-1 activity, significantly improved the myeloablation-related mortality and promoted rapid hematopoietic recovery after HSCT through the induction of hematopoiesis-promoting factors. The ability of a PAI-1 inhibitor to enhance hematopoietic regeneration was abolished when tPA-deficient mice were used as recipients, thus indicating that PAI-1 represses tPA-dependent hematopoietic regeneration. The PAI-1 inhibitor not only accelerated the expansion of the donor HSCs during the early-stage of regeneration, but also supported long-term hematopoiesis. Our results indicate that the inhibition of PAI-1 activity could be a therapeutic approach to facilitate the rapid recovery and sustained hematopoiesis after HSCT. *STEM CELLS* 2014;32:946–958

INTRODUCTION

Hematopoietic stem cell transplantation (HSCT) is used as a therapy for patients who suffer from hematological malignancies. In general, such patients are myeloablated by chemotherapy and/or radiotherapy to eradicate the deranged host hematopoietic system, followed by transplantation of healthy donor-derived hematopoietic cells [1]. However, due to a low engraftment efficiency and delayed bone marrow (BM) reconstitution, these patients occasionally suffer from severe immunodeficiency, thus leading to an increased susceptibility to serious infectious diseases, and therefore, to a high-risk of transplant-related death [2]. The establishment of an efficient strategy to improve the recovery and sustain hematopoiesis is a goal in the treatment of patients undergoing HSCT.

The fibrinolytic pathway breaks down fibrin clots in the blood, and plasmin plays a central role in this process [3]. The proenzyme plasminogen (Plg) is produced from the liver and

circulates in the blood stream. Under certain circumstances, such as wound healing, Plg is proteolytically converted into the active enzyme plasmin by tissue-type plasminogen activator (tPA), which is released from endothelial cells [4]. The blood also contains negative regulators of the fibrinolysis pathway, including plasminogen activator inhibitor-1 (PAI-1). The production of plasmin from plasminogen is thus regulated by a balance between activator molecules (e.g., tPA) and their inhibitors (e.g., PAI-1) [4, 5]. Therefore, inhibiting the PAI-1 activity is expected to accelerate the activation of the tPA-mediated fibrinolytic pathway.

Recently, Hattori and colleagues demonstrated that the fibrinolytic pathway regulates hematopoietic regeneration [6, 7]. They showed that the deletion of the *Plg* gene impaired the entry of quiescent HSCs into the cell cycle and delayed hematopoietic regeneration. In contrast, the activation of Plg by the exogenous administration of recombinant tPA promoted HSC proliferation and differentiation

^aDivision of Hematopoiesis, Research Center for Regenerative Medicine, ^bDepartment of Hematology and Oncology, ^cDepartment of Cell Transplantation and Regenerative Medicine; Tokai University School of Medicine, Isehara, Kanagawa, Japan; ^dMolecular Medicine and Therapy, United Centers for Advanced Research and Translational Medicine, Tohoku University Graduate School of Medicine, Sendai, Miyagi, Japan; ^eService de Nephrologie, Universite Catholique de Louvain, Brussels, Belgium

Correspondence: Takashi Yahata, Ph.D., Tokai University School of Medicine, Isehara, Kanagawa 259-1193, Japan. Telephone: 81-463-1121; Fax: 81-463-92-4750; e-mail: yahata@is.icc.u-tokai.ac.jp; or Kiyoshi Ando, M.D., Ph.D., Tokai University School of Medicine, Isehara, Kanagawa 259-1193, Japan. Telephone: 81-463-1121; Fax: 81-463-92-4750; e-mail: andok@keyaki.cc.u-tokai.ac.jp

Received August 12, 2013; accepted for publication October 3, 2013; first published online in *STEM CELLS EXPRESS* October 24, 2013.

© AlphaMed Press
1066-5099/2014/\$30.00/0

<http://dx.doi.org/10.1002/stem.1577>